

# Let SQL Drive the XQuery Workhorse

## (XQuery Join Graph Isolation)

Torsten Grust

Manuel Mayr

Jan Rittinger

Eberhard Karls Universität Tübingen  
Tübingen, Germany

torsten.grust | manuel.mayr | jan.rittinger@uni-tuebingen.de

### ABSTRACT

A purely relational account of the true XQuery semantics can turn any relational database system into an XQuery processor. Compiling nested expressions of the fully compositional XQuery language, however, yields odd algebraic plan shapes featuring scattered distributions of join operators that currently overwhelm commercial SQL query optimizers.

This work rewrites such plans before submission to the relational database back-end. Once cast into the shape of join graphs, we have found off-the-shelf relational query optimizers—the B-tree indexing subsystem and join tree planner, in particular—to cope and even be autonomously capable of “reinventing” advanced processing strategies that have originally been devised specifically for the XQuery domain, *e.g.*, XPath step reordering, axis reversal, and path stitching. Performance assessments provide evidence that relational query engines are among the most versatile and efficient XQuery processors readily available today.

### Categories and Subject Descriptors

H.2.4 [Database Management]: Systems—*Query Processing, Relational Databases*

## 1. INTRODUCTION

SQL query optimizers strive to produce query plans whose primary components are *join graphs*—bundles of relations interconnected by join predicates—while a secondary, peripheral *plan tail* performs further filtering, grouping, and sorting. Plans of this particular type are subject to effective optimization strategies that, taking into account the available indexes and applicable join methods, derive equivalent join trees, ideally with a left-deep profile to enable pipelining. For more than 30 years now, relational query processing infrastructure has been tuned to excel at the evaluation of plans of this shape.

SQL’s rather rigid syntactical block structure facilitates its compilation into join graphs. The compilation of *truly com-*

Permission to make digital or hard copies of all or part of this work for personal or classroom use is granted without fee provided that copies are not made or distributed for profit or commercial advantage and that copies bear this notice and the full citation on the first page. To copy otherwise, to republish, to post on servers or to redistribute to lists, requires prior specific permission and/or a fee.

EDBT 2010, March 22–26, 2010, Lausanne, Switzerland.

Copyright 2010 ACM 978-1-60558-945-9/10/0003 ...\$10.00

|                      |   |  |       |
|----------------------|---|--|-------|
| <i>Expr</i>          | → | for <i>\$VarName</i> in <i>Expr</i> return <i>Expr</i> |       |
|                      |   | let <i>\$VarName</i> := <i>Expr</i> return <i>Expr</i> |       |
|                      |   | <i>\$VarName</i>                                       |       |
|                      |   | if ( <i>BoolExpr</i> ) then <i>Expr</i> else ()        |       |
|                      |   | doc( <i>StringLiteral</i> )                            |       |
|                      |   | <i>Expr</i> / <i>ForwardAxis</i> <i>NodeTest</i>       |       |
|                      |   | <i>Expr</i> / <i>ReverseAxis</i> <i>NodeTest</i>       |       |
| <i>BoolExpr</i>      | → | <i>Expr</i>  |       |
|                      |   | <i>Expr</i> <i>GeneralComp</i> <i>Expr</i>             |       |
|                      |   | <i>Expr</i> <i>GeneralComp</i> <i>Literal</i>          |       |
| <i>GeneralComp</i>   | → | =   !=   <   <=   >   >=                               | [60]  |
| <i>ForwardAxis</i>   | → | descendant::   following::   ...                       | [73]  |
| <i>ReverseAxis</i>   | → | parent::   ancestor::   ...                            | [76]  |
| <i>NodeTest</i>      | → | <i>KindTest</i>   <i>NameTest</i>                      | [78]  |
| <i>Literal</i>       | → | <i>NumericLiteral</i>   <i>StringLiteral</i>           | [85]  |
| <i>VarName</i>       | → | <i>QName</i>   | [88]  |
| <i>StringLiteral</i> | → | "..."  | [144] |

Figure 1: Relevant XQuery “workhorse” subset (source language). Annotations in [·] refer to the grammar rules in [4, Appendix A].

*positional* expression-oriented languages like XQuery, however, may yield plans of unfamiliar shape [12]. The arbitrary nesting of *for* loops (iteration over ordered item sequences), in particular, leads to plans in which join and sort operators as well as duplicate elimination occur throughout. Such plans overwhelm current commercial SQL query optimizers: the numerous occurrences of sort operators block join operator movement, effectively separate the plan into fragments, and ultimately lead to unacceptable query performance.

Here, we propose a plan rewriting procedure that derives join graphs from plans generated by the XQuery compiler described in [12]. The XQuery order and duplicate semantics are preserved. The resulting plan may be equivalently expressed as a single *SELECT-DISTINCT-FROM-WHERE-ORDER BY* block to be submitted for execution by an off-the-shelf RDBMS. The database system then evaluates this query over a schema-oblivious tabular encoding of XML documents to compute the encoding of the resulting XML node sequence (which may then be serialized to yield the expected XML text).

In this work we restrict ourselves to the XQuery Core fragment, defined by the grammar in Fig. 1, that admits the orthogonal nesting of *for* loops over XML node sequences (of type *node()\**), supports the 12 axes of XQuery’s *full axis* feature, arbitrary XPath name and kind tests, as well as general comparisons in conditional expressions whose *else* clause yields the empty sequence (). As such, the fragment is considerably more expressive than the widely considered

*twig* queries [6, 7] and can be characterized as XQuery’s data-bound “workhorse”: XQuery uses this fragment to collect, filter, and join nodes from participating XML documents before further processing steps (grouping, tree construction) are performed. Others have described the data needs of a query in terms of tree patterns [3], here we use a fragment of the XQuery language itself.

Isolating the join graph implied by the input XQuery expression lets the relational database query optimizer face a problem known inside out despite the source language not being SQL: in essence, the join graph isolation process emits a bundle of self-joins over the tabular XML document encoding connected by conjunctive equality and range predicates. Most interestingly, we have found relational query optimizers to be autonomously capable of translating these join graphs into join trees that, effectively, (1) perform cost-based shuffling of the evaluation order of XPath location steps and predicates, (2) exploit XPath axis reversal (*e.g.*, trade *ancestor* for *descendant*), and (3) break up and stitch complex path expressions. In recent years, all of these have been described as specific evaluation and optimization techniques in the XPath and XQuery domain [6, 16, 18]—here, instead, they are the *automatic result* of join tree planning solely based on the availability of vanilla B-tree indexes and associated statistics. The resulting plans fully exploit the relational database kernel infrastructure, effectively turning the RDBMS into an XQuery processor that can perfectly cope with large XML instances (of size 100 MB and beyond).

Join graph isolation is an essential part of *Pathfinder*<sup>1</sup>—a full-fledged compiler for the complete XQuery language specification that is targeting relational database back-ends. For all of these back-ends we observed significant query execution time improvements for popular XQuery benchmarks, *e.g.*, XMark or the query section of TPoX [17, 22]. One particular back-end is MonetDB. MonetDB/XQuery [5]—the combination of *Pathfinder* and MonetDB—uses the techniques described in this work to robustly detect value-based joins regardless of syntactic query variation. The role of join graph isolation becomes even more important in the upcoming version of MonetDB/XQuery: join graphs are the starting point for runtime query optimization [2].

We start to explore this form of XQuery join graph isolation in Section 2 where we review the compiler’s algebraic target language, tabular XML document encodings, and join-based compilation rules for XPath location steps, nested *for* loops, and conditionals. The rewriting procedure of Section 3 then isolates the join graphs buried in the initial compiled plans. Cast in terms of an SQL query, IBM DB2 V9’s relational query processor is able turn these graphs into join trees which, effectively, implement a series of otherwise XQuery- and XPath-specific optimizations. A further quantitative experimental assessment demonstrates that DB2 V9’s built-in pureXML™ XQuery processor currently faces a serious challenger with its relational self if the latter is equipped with the join graph-isolating compiler (Section 4). Sections 5 and 6 conclude this paper with reviews of related efforts and work in flux.

## 2. JOIN-BASED XQUERY SEMANTICS

To prepare join graph isolation, the compiler translates the XQuery fragment of Fig. 1 into intermediate DAG-shaped

<sup>1</sup><http://www.pathfinder-xquery.org/>

**Table 1: Table algebra dialect (compilation target language).**

| Operator  | Semantics   |
|---|---|
| $\wp_{b_1, b_2}$  | plan root (serialize column $b_1$ by order in $b_2$ ) |
| $\pi_{a_1: b_1, \dots, a_n: b_n}$   | project onto columns $b_i$ , rename $b_i$ into $a_i$  |
| $\sigma_p$  | select rows that satisfy predicate $p$                |
| $\bowtie_p$   | join with predicate $p$                               |
| $\times$  | Cartesian product                                     |
| $\delta$  | eliminate duplicate rows                              |
| $@_{a:c}$   | attach column $a$ containing constant value $c$       |
| $\#_a$  | attach arbitrary unique row id in column $a$          |
| $\varrho_{a:(b_1, \dots, b_n)}$   | attach row rank in $a$ (in $b_1, \dots, b_n$ order)   |
| <b>doc</b>  | XML document encoding table                           |
| $\begin{array}{ c c } \hline a & b \\ \hline c_1 & c_2 \\ \hline \end{array}$ | singleton literal table (with columns $a, b$ )        |

```
<open_auction id="1">
  <initial>
    15
  </initial>
  <bidder>
    <time>18:43</time>
    <increase>
      4.20
    </increase>
  </bidder>
</open_auction>
```

| pre | size | level | kind | name     | value | data |
|-----|------|-------|------|----------|-------|------|
| 0   | 9    | 0     | DOC  | au...xml |       |      |
| 1   | 8    | 1     | ELEM | open_... |       |      |
| 2   | 0    | 2     | ATTR | id       | 1     | 1.0  |
| 3   | 1    | 2     | ELEM | initial  | 15    | 15.0 |
| 4   | 0    | 3     | TEXT |          | 15    | 15.0 |
| 5   | 4    | 2     | ELEM | bidder   |       |      |
| 6   | 1    | 3     | ELEM | time     | 18:43 |      |
| 7   | 0    | 4     | TEXT |          | 18:43 |      |
| 8   | 1    | 3     | ELEM | incre... | 4.20  | 4.2  |
| 9   | 0    | 4     | TEXT |          | 4.20  | 4.2  |

**Figure 2: Encoding of the infoset of XML document auction.xml. Column data carries the nodes’ typed decimal values.**

plans over the logical table algebra of Table 1. This particularly simple algebra dialect has been designed to match the capabilities of SQL query engines: operators consume tables (not relations) and duplicate row elimination is explicit (in terms of  $\delta$ ). The row rank operator  $\varrho_{a:(b_1, \dots, b_n)}$  exactly mimics SQL:1999’s `RANK() OVER (ORDER BY  $b_1, \dots, b_n$ ) AS a` and is primarily used to account for XQuery’s pervasive sequence order notion. The attach operator  $@_{a:c}(e)$  abbreviates  $e \times \begin{array}{|c|} \hline a \\ \hline c \\ \hline \end{array}$ , where the right-hand side argument denotes a singleton literal table. Operator  $\wp$  marks the serialization point at the root of the plan DAG, delivering those rows that encode the resulting XML node sequence. Below we will see how the join operator  $\bowtie$  assumes a central role in the translation of XPath location steps, *for* loops, and conditional expressions.

### 2.1 XML Infoset Encoding

An encoding of persistent XML infosets is provided via the designated table **doc**. In principle, any schema-oblivious node-based encoding of XML nodes that admits the evaluation of XPath node tests and axis steps fits the bill (*e.g.*, *ORDPATH* [19]). The following uses one such row-based format in which, for each node  $v$ , key column **pre** holds  $v$ ’s unique document order rank to form—together with columns **size** (number of nodes in subtree below  $v$ ) and **level** (length of path from  $v$  to its document root node)—an encoding of the XML tree structure (Fig. 2 and [13]). XPath kind and name tests access columns **kind** and **name**—multiple occurrences of value **DOC** in column **kind** indicate that table **doc** hosts several trees, distinguishable by their document URIs (in column **name**). For nodes with **size**  $\leq 1$ , table **doc** supports value-based node access in terms of two columns that carry

the node’s untyped string value [9, § 3.5.2] and, if applicable, the result of a cast to type `xs:decimal`<sup>2</sup> (columns `value` and `data`, respectively). This tabular XML infoset representation may be efficiently populated (during a single parsing pass over the XML document text) and serialized again (via a table scan in `pre` order).

| $n$                       | $kindt(n)$               | $n$                        | $namet(n)$            |
|---------------------------|--------------------------|----------------------------|-----------------------|
| <code>element(,)</code>   | <code>kind = ELEM</code> | <code>element(t,)</code>   | <code>name = t</code> |
| <code>attribute(,)</code> | <code>kind = ATTR</code> | <code>attribute(t,)</code> | <code>name = t</code> |
| <code>text()</code>       | <code>kind = TEXT</code> | <code>text()</code>        | <code>true</code>     |
| $\vdots$                  | $\vdots$                 | $\vdots$                   | $\vdots$              |

| $\alpha$                | $axis(\alpha)$   |
|-------------------------|--|
| <code>child</code>      | $pre_o < pre \leq pre_o + size_o \wedge level_o + 1 = level$ |
| <code>descendant</code> | $pre_o < pre \leq pre_o + size_o$                            |
| <code>ancestor</code>   | $pre < pre_o \leq pre + size$                                |
| <code>following</code>  | $pre_o + size_o < pre$                                       |
| $\vdots$                | $\vdots$   |

**Figure 3: Predicates implementing the semantics of XPath kind and name tests—expressed in sequence type syntax [4, § 2.5.3]—and axes (excerpt).  $\circ$  marks the properties of the context node(s).**

## 2.2 XPath Location Steps

Further, this encoding has already been shown to admit the efficient join-based evaluation of location steps  $\alpha::n$  along all 12 XPath axes  $\alpha$  [13]. While the structural node relationship expressed by  $\alpha$  maps into a conjunctive range join predicate  $axis(\alpha)$  over columns `pre`, `size`, `level`, the step’s kind and/or name test  $n$  yields equality predicates over kind and name (Fig. 3). Consider the three-step path  $Q_0 = doc("auction.xml")/descendant::bidder/child::* /child::text()$  over the document of Fig. 2. To perform the final `child::text()` step, which will have context elements `time` and `increase`, the database system evaluates a join between the document encoding and the step’s context nodes (the query yields the `pre` ranks of the two resulting text nodes):

$$\pi_{\text{item:pre}} \left( \sigma_{\substack{kindt(\text{text}()) \wedge \\ namet(\text{text}())}}^{(doc)} \bowtie_{axis(\text{child})} \begin{array}{|c|c|c|c|} \hline pre_o & size_o & level_o & \dots \\ \hline 6 & 1 & 3 & \vdots \\ \hline 8 & 1 & 3 & \vdots \\ \hline \end{array} \right) = \begin{array}{|c|} \hline \text{item} \\ \hline 7 \\ \hline 9 \\ \hline \end{array}.$$

With their ability to perform range scans, regular B-tree indexes, built over table `doc`, perfectly support this style of location step evaluation [13].

## 2.3 A Loop-Lifting XQuery Compiler

From [12] we adopt a view of the dynamic XQuery semantics, *loop lifting*, that revolves around the `for` loop as the core language construct. Any subexpression  $e$  is considered to be iteratively evaluated inside its innermost enclosing `for` loop. For the XQuery fragment of Fig. 1, each iterated evaluation of  $e$  yields a (possibly empty) ordered sequence of nodes. To reflect this, we compile  $e$  into an algebraic plan that returns a ternary table with schema `iter|pos|item`: a row  $[i, p, v]$  indicates that, in iteration  $i$ , the evaluation of

$e$  returned a sequence containing a node with `pre` rank  $v$  at sequence position  $p$ .

The inference rules `DOC`, `DDO`, `STEP`, `IF`, `VALCOMP`, `COMP`, `LET`, `FOR`, and `VAR` (taken from [12] and reproduced in Appendix A) form a *compositional* algebraic compilation scheme for the XQuery dialect of Fig. 1. The rule set expects to see the input query after XQuery Core normalization: the enforcement of duplicate node removal and document order after XPath location steps (via the application of `fs:distinct-doc-order()`, abbreviated to `fs:ddo()` in the following) and the computation of effective Boolean values in conditionals (via `fn:boolean()`) is explicit [9, § 4.2.1 and § 3.4.3].

Changing the XML infoset encoding in Section 2.1 or the XPath location step implementation in Section 2.2 requires a local modification only: the adjustment of the inference rules `DOC` and `STEP` in Appendix A.<sup>3</sup>

## 2.4 The Compositionality Threat

To obtain an impression of typical plan features, we compile

$$doc("auction.xml") /descendant::open_auction[bidder] . \quad (Q_1)$$

After XQuery Core normalization, this query reads

```
for $x in fs:ddo(doc("auction.xml"))
  /descendant::open_auction)
return if (fn:boolean(fs:ddo($x/child::bidder)))
  then $x else () .
```

Fig. 4 shows the initial plan for  $Q_1$ . Since the inference rules of Fig. 13 implement a *fully compositional* compilation scheme, we can readily identify how the subexpressions of  $Q_1$  contribute to the overall plan (to this end, observe the gray plan sections all of which yield tables with columns `iter|pos|item`). XQuery is a functional expression-oriented language in which subexpressions are stacked upon each other to form complex queries. The tall plan profile with its stacked sections—reaching from a single instance of table `doc` (serving all node references) to the serialization point  $\varphi$ —directly reflects this orthogonal nesting of expressions.

Note, though, how this artifact of both, compositional language and compilation scheme, leads to plans whose shapes differ considerably from the ideal *join graph + plan tail* we have identified earlier. Instead, join operators occur in sections distributed all over the plan. A similar distribution can be observed for the blocking operators  $\delta$  and  $\rho$  (duplicate elimination and row ranking). This is quite unlike the algebraic plans produced by SQL `SELECT-FROM-WHERE` block compilation.

The omnipresence of blocking operators obstructs join operator movement and planning and leads industrial-strength optimizers, *e.g.*, IBM DB2 UDB V9, to execute the plan in stages that read and then again materialize temporary tables. In the following we will therefore follow a different route and instead *reshape* the plan into a join graph that becomes subject to efficient one-shot execution by the SQL database back-end. (Section 4 will show that join graph isolation for  $Q_1$  improves the evaluation time by a factor of 5.)

<sup>3</sup>MonetDB/XQuery, *e.g.*, uses a general structural join operator as a replacement for  $\bowtie_{axis(\alpha)}$  in Rule `STEP`. After join graph isolation, these structural join operators are transformed into physical loop-lifted staircase join primitives [5].

<sup>2</sup>In the interest of space, we omit a discussion of the numerous further XML Schema built-in data types.



**Table 2: Top-down inference of property *icols* for the input(s) of operator  $\otimes$ .**

| Operator $\otimes$                   | Inferred property <i>icols</i> of input(s) of $\otimes$                                 |
|--------------------------------------|---|
| $\varphi_{b_1, b_2}(e)$              | $e.icols \leftarrow \{b_1, b_2\}$   |
| $\pi_{a_1: b_1, \dots, a_n: b_n}(e)$ | $e.icols \leftarrow e.icols \cup \{b_i \mid a_i \in (icols \cap \{a_1, \dots, a_n\})\}$ |
| $\sigma_p(e)$                        | $e.icols \leftarrow e.icols \cup icols \cup cols(p)$                                    |
| $e_1 \bowtie_p e_2$                  | $e_{1,2}.icols \leftarrow e_{1,2}.icols \cup ((icols \cup cols(p)) \cap cols(e_{1,2}))$ |
| $e_1 \times e_2$                     | $e_{1,2}.icols \leftarrow e_{1,2}.icols \cup (icols \cap cols(e_{1,2}))$                |
| $\delta(e)$                          | $e.icols \leftarrow e.icols \cup icols$   |
| $@_{a:c}(e)$                         | $e.icols \leftarrow e.icols \cup (icols \setminus \{a\})$                               |
| $\#_a(e)$                            | $e.icols \leftarrow e.icols \cup (icols \setminus \{a\})$                               |
| $\varrho_{a:(b_1, \dots, b_n)}(e)$   | $e.icols \leftarrow e.icols \cup (icols \setminus \{a\}) \cup \{b_1, \dots, b_n\}$      |
| doc                                  | —   |
| $\frac{a \ b}{c_1 \ c_2}$            | —   |

**Table 3: Bottom-up inference of property *const* for operator  $\otimes$ .**

| Operator $\otimes$                   | Inferred property <i>const</i> of $\otimes$               |
|--------------------------------------|---|
| $\varphi_{b_1, b_2}(e)$              | $const \leftarrow e.const$                                |
| $\pi_{a_1: b_1, \dots, a_n: b_n}(e)$ | $const \leftarrow \{a_i = c \mid (b_i = c) \in e.const\}$ |
| $\sigma_p(e)$                        | $const \leftarrow e.const$                                |
| $e_1 \bowtie_p e_2$                  | $const \leftarrow e_1.const \cup e_2.const$               |
| $e_1 \times e_2$                     | $const \leftarrow e_1.const \cup e_2.const$               |
| $\delta(e)$                          | $const \leftarrow e.const$                                |
| $@_{a:c}(e)$                         | $const \leftarrow e.const \cup \{a = c\}$                 |
| $\#_a(e)$                            | $const \leftarrow e.const$                                |
| $\varrho_{a:(b_1, \dots, b_n)}(e)$   | $const \leftarrow e.const$                                |
| doc                                  | $const \leftarrow \emptyset$                              |
| $\frac{a \ b}{c_1 \ c_2}$            | $const \leftarrow \{a = c_1, b = c_2\}$                   |

**Table 4: Bottom-up inference of property *key* for operator  $\otimes$ .**

| Operator $\otimes$                   | Inferred property <i>key</i> of $\otimes$  |
|--------------------------------------|--|
| $\varphi_{b_1, b_2}(e)$              | $key \leftarrow e.key$   |
| $\pi_{a_1: b_1, \dots, a_n: b_n}(e)$ | $key \leftarrow \{\{a_i \mid b_i \in k\} \mid k \in e.key, k \subseteq \{b_1, \dots, b_n\}\}$  |
| $\sigma_p(e)$                        | $key \leftarrow e.key$   |
| $e_1 \bowtie_{a=b} e_2$              | $key \leftarrow \{k_1 \mid \{b\} \in e_2.key, k_1 \in e_1.key\}$<br>$\cup \{k_2 \mid \{a\} \in e_1.key, k_2 \in e_2.key\}$<br>$\cup \{(k_1 \setminus \{a\}) \cup k_2 \mid \{b\} \in e_2.key, k_1 \in e_1.key, k_2 \in e_2.key\}$<br>$\cup \{k_1 \cup (k_2 \setminus \{b\}) \mid \{a\} \in e_1.key, k_1 \in e_1.key, k_2 \in e_2.key\}$ |
| $e_1 \bowtie_p e_2$                  | $key \leftarrow \{k_1 \cup k_2 \mid k_1 \in e_1.key, k_2 \in e_2.key\}$  |
| $e_1 \times e_2$                     | $key \leftarrow \{k_1 \cup k_2 \mid k_1 \in e_1.key, k_2 \in e_2.key\}$  |
| $\delta(e)$                          | $key \leftarrow e.key \cup \{cols(e)\}$  |
| $@_{a:c}(e)$                         | $key \leftarrow e.key$   |
| $\#_a(e)$                            | $key \leftarrow e.key \cup \{\{a\}\}$  |
| $\varrho_{a:(b_1, \dots, b_n)}(e)$   | $key \leftarrow e.key$<br>$\cup \{\{a\} \cup (k \setminus \{b_1, \dots, b_n\}) \mid k \in e.key, k \cap \{b_1, \dots, b_n\} \neq \emptyset\}$  |
| doc                                  | $key \leftarrow \{\{pre\}\}$   |
| $\frac{a \ b}{c_1 \ c_2}$            | $key \leftarrow \{\{a\}, \{b\}, \{a, b\}\}$  |

**Table 5: Top-down inference of Boolean property *set* for the input(s) of operator  $\otimes$ .**

| Operator $\otimes$                   | Inferred property <i>set</i> of the input(s) of $\otimes$ |
|--------------------------------------|---|
| $\varphi_{b_1, b_2}(e)$              | $e.set \leftarrow false$                                  |
| $\pi_{a_1: b_1, \dots, a_n: b_n}(e)$ | $e.set \leftarrow e.set \wedge set$                       |
| $\sigma_p(e)$                        | $e.set \leftarrow e.set \wedge set$                       |
| $e_1 \bowtie_p e_2$                  | $e_{1,2}.set \leftarrow e_{1,2}.set \wedge set$           |
| $e_1 \times e_2$                     | $e_{1,2}.set \leftarrow e_{1,2}.set \wedge set$           |
| $\delta(e)$                          | $e.set \leftarrow e.set \wedge true$                      |
| $@_{a:c}(e)$                         | $e.set \leftarrow e.set \wedge set$                       |
| $\#_a(e)$                            | $e.set \leftarrow false$                                  |
| $\varrho_{a:(b_1, \dots, b_n)}(e)$   | $e.set \leftarrow e.set \wedge set$                       |
| doc                                  | —   |
| $\frac{a \ b}{c_1 \ c_2}$            | —   |

$$\begin{array}{c}
\frac{}{q \times \frac{a \ b}{c_1 \ c_2} \rightarrow @_{a:c}(q)} (1) \quad \frac{}{\pi_{a_1, \dots, a_n}(\pi_{b_1, \dots, b_m}(q)) \rightarrow \pi_{a_1, \dots, a_n}(q)} (2) \quad \frac{\{a = c, b = c\} \subseteq const}{q_1 \bowtie_{a=b} q_2 \rightarrow q_1 \times q_2} (3) \\
\frac{a \notin icols}{@_{a:c}(q) \rightarrow q} (4) \quad \frac{a \notin icols}{\varrho_{a:(b_1, \dots, b_n)}(q) \rightarrow q} (5) \quad \frac{a \notin icols}{\#_a(q) \rightarrow q} (6) \quad \frac{icols \neq \emptyset \quad \{a_1, \dots, a_n\} \setminus icols \neq \emptyset}{\pi_{a_1, \dots, a_n}(q) \rightarrow \pi_{\{a_1, \dots, a_n\} \cap icols}(q)} (7) \\
\frac{const \setminus \{b_1, \dots, b_n\} \neq \emptyset}{\varrho_{a:(b_1, \dots, b_n)}(q) \rightarrow \varrho_{a:(b_1, \dots, b_n) \setminus const}(q)} (8) \quad \frac{}{\varrho_{a:(b)}(q) \rightarrow \pi_{a:b, cols}(q)} (9) \quad \frac{\otimes \in \{\sigma_p, \delta, @, \#\} \quad a \notin cols(p)}{\otimes(\varrho_{a:(b_1, \dots, b_n)}(q)) \rightarrow \varrho_{a:(b_1, \dots, b_n)}(\otimes(q))} (10) \\
\frac{}{\pi_{a, c_1, \dots, c_m}(\varrho_{a:(b_1, \dots, b_n)}(q)) \rightarrow \varrho_{a:(b_1, \dots, b_n)}(\pi_{b_1, \dots, b_n, c_1, \dots, c_m}(q))} (11) \quad \frac{\otimes \in \{\bowtie_p, \times\} \quad a \notin cols(p)}{\varrho_{a:(b_1, \dots, b_n)}(q_1) \otimes q_2 \rightarrow \varrho_{a:(b_1, \dots, b_n)}(q_1 \otimes q_2)} (12) \\
\frac{}{\varrho_{a:(\dots, b_i, \dots)}(\varrho_{b_i:(c_1, \dots, c_m)}(q)) \rightarrow \varrho_{a:(\dots, b_{i-1}, c_1, \dots, c_m, b_{i+1}, \dots)}(\varrho_{b_i:(c_1, \dots, c_m)}(q))} (13) \\
\frac{set}{\delta(q) \rightarrow q} (14) \quad \frac{const \setminus icols \neq \emptyset}{\delta(q) \rightarrow \delta(\pi_{cols(q) \setminus (const \setminus icols)}(q))} (15) \quad \frac{\neg set \quad \otimes \notin \{\delta, \varrho\} \quad k \in key \quad k \subseteq icols}{\otimes(q) \rightarrow \delta(\pi_{icols}(\otimes(q)))} (16) \\
\frac{\otimes \in \{\pi, \sigma_p, @\} \quad a \in cols(q_1)}{\otimes(q_1) \bowtie_{a=b} q_2 \rightarrow \otimes(q_1 \bowtie_{a=b} q_2)} (17) \quad \frac{\otimes \in \{\bowtie_p, \times\} \quad a \in cols(q_2)}{(q_1 \otimes q_2) \bowtie_{a=b} q_3 \rightarrow q_1 \otimes (q_2 \bowtie_{a=b} q_3)} (18) \quad \frac{\{a\} \in key \quad q_1 \Rightarrow q_2 \quad q_2 \Rightarrow q_1}{q_1 \bowtie_{a=a} q_2 \rightarrow q_1} (19)
\end{array}$$

**Figure 5: Join graph isolation transformation (for a rule  $lhs \rightarrow rhs$ , the properties *icols*, *const*, *set*, and *key* denote the properties of *lhs*).**

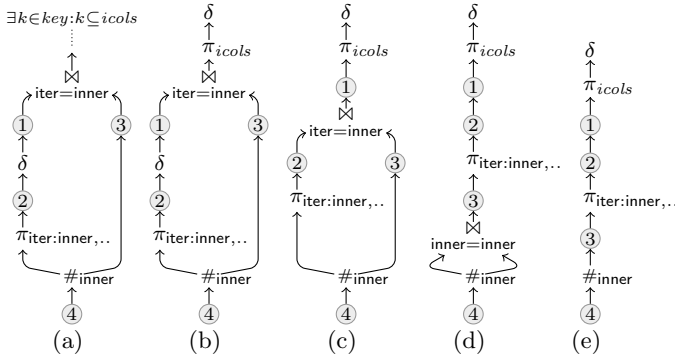


**Figure 6: Moving duplicate elimination into the plan tail and join push-down (stages shown left to right).**

goal-directed applications of the rewrite rules in Fig. 5.<sup>4</sup> Note how the rules’ premises inspect the inferred plan properties, as described above. The subgoals either strictly move  $\varrho$  and  $\delta$  towards the plan tail or push equi-joins ( $\bowtie_{a=b}$ ) down into the plan. In addition to these three main goals, “house cleaning” is performed by rules defined to simplify or remove operators (Rules (1–8), (14), and (15)). House-cleaning in Fig. 4, *e.g.*, leads to the removal of the cross product and its rhs subtree (application of Rules (4)–(1)–(4)) as well as the removal of unreferenced rank operators (Rule (5)). While house-cleaning is performed whenever necessary, goal  $\textcircled{a}$  is pursued before the two other subgoals.

$\textcircled{a}$  **Establish a single  $\varrho$  operator in the plan tail.** A *single* instance of the row ranking operator  $\varrho$  suffices to correctly implement the sequence and document order requirements of the overall plan. To this end, Rule (9) trades a  $\varrho$  for a projection if  $\varrho$  ranks over a single column. For the compilation Rules DDO and STEP, which introduce single-column row rankings ( $\varrho_{\text{pos}:(\text{item})}$ ), this effectively means that document order determines sequence order—which is indeed the case for the result of XPath location steps and `fs:ddo()`. All other instances of  $\varrho$  ( $\varrho_{\text{pos}_1:(\text{sort},\text{pos})}$ , introduced by FOR) are moved towards the plan tail via Rules (10–12). The premises of Rules (10) and (12) are no obstacle here: for the XQuery fragment of Fig. 1, the compiler does not emit predicates over sequence positions (column `pos`). Once arrived in the plan tail, Rule (13) splices the ranking criteria of adjacent  $\varrho$  operators. Rule (5) finally removes all but the topmost instance of  $\varrho$ .

$\textcircled{b} + \textcircled{c}$  **Establish a single  $\delta$  operator in the plan tail + join push-down and removal.** Duplicate elimination relocation and join push-down and removal are intertwined. Fig. 6—an abstract representation of Fig. 4—illustrates the stages of this process (the  $\circ$  represent plan sections). These subgoals target and ultimately delete the equi-joins introduced by the compilation Rules STEP, COMP, IF, and FOR (the latter is in focus here).

A join of this type preserves the keys established by `#inner` and thus emits unique rows. The introduction of a new  $\delta$  instance at the top of the plan fragment thus does not alter the

plan semantics (Rule (16), see Figures 6(a) and (b)). This renders the original instance of  $\delta$  obsolete as duplicate elimination now occurs upstream (Rule (14), Fig. 6(c)). The following stages push the join towards the plan base, leaving a trail of plan sections that formerly occurred in the join input branches (Rules (17–18), Figures 6(c) and (d)). Rule (19) detects that the join has degenerated into a key join over identical inputs and thus may be removed (Fig. 6(e)). Finally, this renders the remaining instance of `#inner` obsolete (column `inner` not referenced, Rule (6)).

**Rewrite rules guarantee progress and termination.** The house-cleaning rules (Rules (1–8), (14), and (15)) either remove an operator or restrict its arguments. The rules affecting rank operators (Rules (5) and (8–13)) pull-up rank operators through any other operator and result in at most a single rank operator at the plan root (see discussion of subgoal  $\textcircled{a}$ ). The compilation rules in Appendix A ensure that the position information forms a key at the plan root. Rule (16) thus ensures that a single distinct operator sits in the plan tail. With both distinct and rank operators out of the way, Rules (17–18) push down equi-joins until either an instance of `#` is reached or Rule (19) applies (see discussion on subgoal  $\textcircled{c}$ ). Once `#inner` becomes obsolete because column `inner` is no longer referenced by any equi-join, Rule (6) removes `#inner` and thus allows the remaining equi-joins to be pushed further done until no more rules are applicable.<sup>5</sup>

### 3.3 XQuery in the Guise of SQL SFW-Blocks

Fig. 7 depicts the isolation result for Query  $Q_1$  (original plan shown in Fig. 4). The new plan features a bundle of operators in which—besides instances of  $\pi$ ,  $\sigma$ —the only remaining joins originate from applications of compilation Rule STEP, implementing the semantics of XPath location steps. The joins consume rows from the XML infoset encoding table `doc` which now is the only shared plan node in the DAG. As desired, we can also identify the plan tail (in the case of  $Q_1$ , no extra row ranking is required since the `descendant::open_auction` step—in column `pre` produced by the topmost  $\pi$  operator—already determine the overall order of the result.)

Quite unlike the initial plans emitted by the compositional compiler, XQuery join graph isolation derives logical query plans that are truly indistinguishable from the algebraic plans produced by a regular SQL translator. We thus let an off-the-shelf relational database back-end *autonomously* take over from here. It is now reasonable to expect the system to excel at the evaluation of the considered XQuery fragment as it will face a familiar workload. (This is exactly what we observe in Section 4.)

Most importantly, the join graphs provide a *complete* description of the input query’s true XQuery semantics but *do not prescribe* a particular order of XPath location step or predicate evaluation. It is our intention to let the RDBMS decide on an evaluation strategy, based on its very own cost model, the availability of join algorithms, and supporting index structures. As a consequence, it suffices to communicate the join graph in form of a standard SQL `SELECT-DISTINCT-FROM-WHERE-ORDER BY`-block—*i.e.*, in a declarative fashion barring any XQuery-specific annotations or similar

<sup>4</sup>In the interest of succinctness, we omit the obvious variants of Rules (12), (17), and (18) in which the lhs and rhs arguments of the commutative operators  $\bowtie_p$  and  $\times$  are swapped, and ignore column renaming in Rules (2), (11), and (17).

<sup>5</sup>Note how adjacent equi-joins might lead to repeated applications of Rule (18). Our implementation avoids such repetition by taking operator argument plan sizes into account.

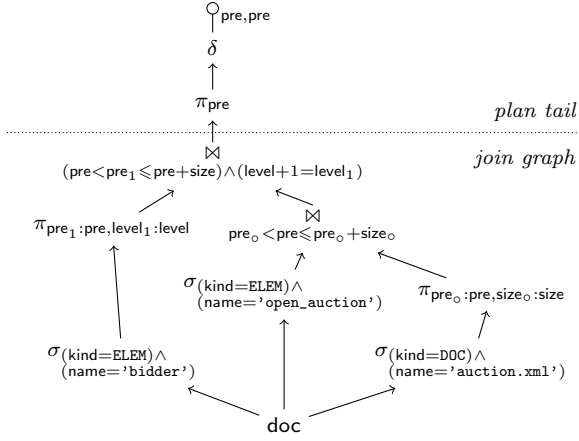


Figure 7: Final plan emitted for  $Q_1$ . The ..... separates the plan tail (above) from the isolated join bundle (three-fold self-join of table doc).

```

SELECT DISTINCT d2.pre
FROM doc AS d1, doc AS d2, doc AS d3
WHERE d1.kind = DOC
  AND d1.name = 'auction.xml'
  AND d2.kind = ELEM
  AND d2.name = 'open_auction'
  AND d2 BETWEEN d1.pre+1 AND d1.pre+d1.size (Q1^SQL)
  AND d3.kind = ELEM
  AND d3.name = 'bidder'
  AND d3 BETWEEN d2.pre+1 AND d2.pre+d2.size
  AND d2.level+1 = d3.level
ORDER BY d2.pre

```

Figure 8: SQL encoding of  $Q_1$ 's join graph.

clues. For Query  $Q_1$ , we thus ship the SQL query  $Q_1^{\text{SQL}}$  (Fig. 8) for execution by the database back-end.

**Plan tail.** The interaction of for loop iteration and sequence order of the final result becomes apparent in the plan tail of the following query (traversing XMark data [22] to return the names of those auction categories in which expensive items were sold at prices beyond \$500):

```

let $a := doc("auction.xml")
for $ca in $a//closed_auction[price > 500],
  $i in $a//item,
  $c in $a//category (Q2)
where $ca/itemref/@item = $i/@id
  and $i/incategory/@category = $c/@id
return $c/name

```

XQuery Core normalization, compilation and subsequent isolation yields the SQL join graph query in Fig. 9 which describes a 12-fold self-join over table doc. Note how the ORDER BY and DISTINCT clauses—which represent the plan tail—reflect the XQuery sequence order and duplicate semantics:

*Order* The nesting of the three for loops in  $Q_2$  principally determines the order of the resulting node sequence: in  $Q_2$ , row variables d2, d4, d5 range over closed\_auction, item, category element nodes, respectively. The document order of the name elements (bound to d12) is least relevant in this example and orders the nodes within each iteration

```

SELECT DISTINCT d12.pre,
  d2.pre AS item1, d4.pre AS item2,
  d5.pre AS item3 (Q2^SQL)
FROM doc AS d1, ..., doc AS d12
WHERE ...
ORDER BY d2.pre, d4.pre, d5.pre, d12.pre

```

Figure 9: SQL encoding of  $Q_2$  (focus on plan tail: order, duplicate removal).

Table 6: B-tree indexes proposed by db2advls.

| Index key columns  | Index deployment  |
|--|---|
|     | XPath node test and axis step, access document node (doc(.))              |
|      | Atomization, value comparison with subsequent/preceding XPath step        |
|   | Serialization support (with columns nvlks in DB2's INCLUDE(.) clause [1]) |
| p:pre, s:pre + size, l:level, k:kind, n:name, v:value, d:data  |   |

of the innermost for loop.

*Duplicates* The XPath location step semantics requires duplicate node removal (row variable d12 appears in the DISTINCT clause). Duplicates are retained, however, across for loop iterations (keys d2.pre, d4.pre, and d5.pre appear in the DISTINCT clause).

## 4. IN LABORATORY WITH IBM DB2 V9 (EXPERIMENTS)

The SQL language subset used to describe the XQuery join graphs—flat self-join chains, simple ordering criteria, and no grouping or aggregation—is sufficiently simple to let any SQL-capable RDBMS assume the role of a back-end for XQuery evaluation. We do *not* rely on SQL/XML functionality, in particular. In what follows, we will observe how IBM DB2 UDB V9 acts as a runtime for the join-graph-isolating compiler. In this context, DB2 V9 appears to be especially interesting, because the system

- (1) has the ability to *autonomously* adapt the design of its physical layer, indexes in particular, in response to a given workload, and
- (2) features the *built-in* XQuery processor pureXML™ which implements a “native” XML document storage and specific primitives for XPath evaluation, but nevertheless relies on the very same database kernel infrastructure. This will provide an insightful point of reference for the performance assessment of Section 4.2.

To provide the RDBMS with complete information about the expected incoming queries, we instructed the compiler to make the semantics of the serialization point  $\circ$  explicit—this adds one extra descendant-or-self::node() step to any Query  $Q$ , originating in its result node sequence:

```
for $x in Q return $x/descendant-or-self::node().
```

This produces all XML nodes required to fully serialize the result (surfacing as the additional topmost self-join in the join plans of Figures 10 and 11).

**Autonomous index design.** For  $Q_2$  as an representative of the prototypical expected query workload, the DB2 automatic design advisor, db2advls [1], suggests the B-tree index

**Table 7: Relevant IBM DB2 plan operators.**

| Operator | Semantics                          | Operator | Semantics                          |
|----------|------------------------------------|----------|------------------------------------|
| RETURN   | Result row delivery                | SORT     | Sort rows (+ dup. row elimination) |
| NLJOIN   | Nested-loop join (left leg: outer) | HSJOIN   | Hash join (left leg: probe)        |
| IXSCAN   | B-tree scan                        | TBSCAN   | Temporary table scan               |
| nlkps    | Index access                       | doc      | XML infoset table access           |

set of Table 6 (with a total size of 300 MB for a 110 MB instance of the XMark `auction.xml` document). Due to the regularity of the emitted SQL code, the utility of the proposed indexes will be high for any XQuery workload that exhibits a significant fraction of XQuery join graphs.

**Partitioned B-tree index support for XQuery.** The majority of the index keys proposed in Table 6 are prefixed with *low cardinality* column(s), e.g., `n`, `nk`, or `nlk`. An XMark XML instance features 77 distinct element tag and attribute names, regardless of the document size. Similar observations apply to the XML node kinds and the typical XML document height. A B-tree that is primarily organized by such a low cardinality column will, in consequence, *partition* the XML infoset encoding into few disjoint node sets [11]. Note how, in a sense, a **name**-prefixed index key leads to a B-tree-based implementation of the *element tag streams*, the principal data access path used in the so-called *twig join* algorithms [6, 7].

The design advisor further suggests an index with key `vnkps` whose `value` column prefix supports atomization and the general value comparisons between (attribute) nodes featured in  $Q_2$ . A B-tree of this type bears some close resemblance with the XPath-specific indexes (`CREATE INDEX ... GENERATE KEY USING XMLPATTERN ... AS SQL VARCHAR(n)`) employed by pureXML™ (Section 4.2).

#### 4.1 XPath Continuations

How exactly does DB2 V9’s query optimizer deploy the indexes proposed by its design advisor companion? An answer to this question can be found through an analysis of the plan trees generated by the optimizer. We have, in fact, observed a few not immediately obvious “tricks” that have found their way into the execution plans. Most of these observations are closely related to query evaluation techniques that have originally been described as XPath-specific [6, 16, 18], outside the relational domain. Since we have transferred all responsibility for the XQuery runtime aspects to the RDBMS, we think this is quite interesting.

The optimized DB2 execution plan found for Query  $Q_1$  of Section 2.4 is shown in Fig. 10. We are reproducing these execution plans in a form closely resembling the output of DB2’s visual explain facility. Nodes in these plans represent operators of DB2’s variant of physical algebra—all operators relevant for the present discussion are introduced in Table 7.

**Path stitching and branching.** Consider the B-tree index with key `nksp`. Due to its `nk` prefix, this index primarily provides support for XPath name and kind tests. In the execution plan for  $Q_1$ , the index is used to access the requested document node (`name = 'auction.xml' ^ kind = DOC`). Additionally, however, the index delivers the infoset

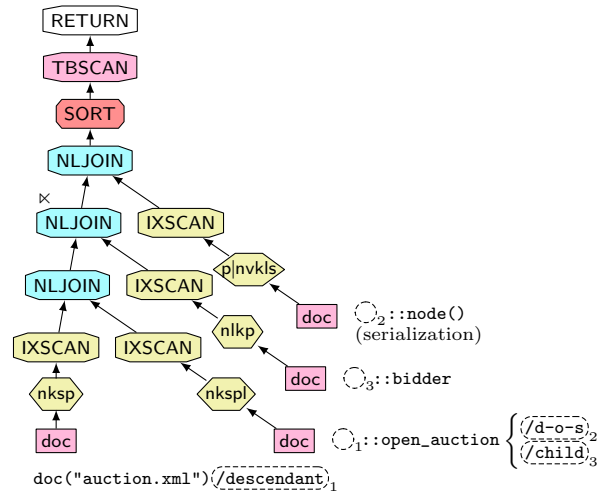


**Figure 10: DB2 V9 execution plan for  $Q_1$  with continuation annotations (d-o-s abbreviates descendant-or-self).**

properties `sp` and thus provides all necessary information to step along the XPath `descendant` axis—namely the interval  $(pre, pre + size]$ , see Fig. 3—from those nodes that have been found during index lookup. In the following, we will denote the result of such index lookups as

$$doc("auction.xml")\{\underline{descendant}\}_1$$

or, generally  $n(\underline{\alpha})_i$  (read: perform the specified node test  $n$ , then prepare a subsequent step along axis  $\alpha$ ). In the execution plan of Fig. 10, the bottom index nested-loop join continues this “half-cooked” step: a lookup in the index `nksp` retrieves columns `nkp` to (1) perform the due name and kind test (`name = 'open_auction' ^ kind = ELEM`) and (2) complete the structural `descendant` axis traversal (check `p` for containment in the  $(pre, pre + size]$  interval obtained in the first half of the step). In the annotated plans, we write  $\bigcirc_1::open\_auction$  (read: resume axis step and perform specified name and kind test). Stitched at the matching continuation points (here: those with subscript 1), we obtain the complete XPath location step again:

$$doc("auction.xml")\{\underline{descendant}\}_1::open\_auction$$

The lookup in index `nksp` further provides the necessary infoset properties to prepare the now current continuations  $\{\underline{descendant-or-self}\}_2$  (columns `sp`) as well as  $\{\underline{child}\}_3$  (columns `sp`). Such continuations with multiple resumption points are the equivalent of the branching nodes discussed in the context of *holistic twig joins* [6].

Given the tailored B-tree index set in Table 6, the DB2 query optimizer consistently manages to select the index access path that provides just the required XML infoset properties. Resuming the `child` continuation at  $\bigcirc_3::bidder$  requires columns `nk` to perform the name and kind test plus columns `pl` to complete the evaluation of the range predicate that implements the `child` step. The semi-join evaluating this path step has its *early-out* flag set (see  $\times$  in Fig. 10) and thus—similar to the original Query  $Q_1$ —applies only a predicate filter. Finally, as anticipated, the plan scans index `p|nvkls` to traverse all nodes in the subtrees below the query’s XML result nodes (resuming from  $\{\underline{descendant-or-self}\}_2$ ).

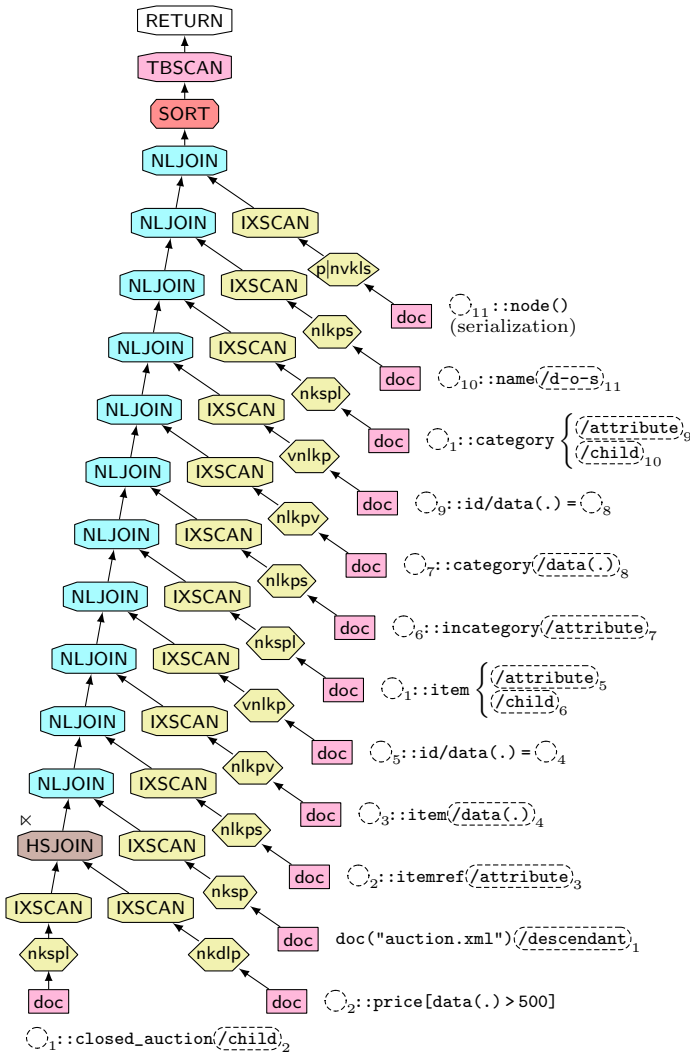


Figure 11: DB2 V9 execution plan for  $Q_2$ .

**XPath step reordering and axis reversal.** Two further phenomena in the execution plans can be explained in terms of the XPath continuation notion. For  $Q_1$ , the order of the XPath location steps specified in the input query did coincide with the join order in the execution plan (access document node of XML instance `auction.xml`, then perform a `descendant::open_auction` step, finally evaluate `child::bidder`). The B-tree index entries provide sufficient context information, however, to allow for arbitrary path processing orders—right-to-left strategies are conceivable as are strategies that start in the middle of a step sequence and then work their way towards the path’s endpoints. The latter can be witnessed in the execution plan of Query  $Q_2$  (Fig. 11).

The plan’s very first index scan over `nkspl` evaluates the name and kind test for elements with tag `closed_auction` before the continuation for resumption point  $\odot_1$  has provided any context node information. The index key columns `spl` are used to prepare the continuation `(/child)_2` which is then immediately resumed by the node test for element `price`. Index `nkdip` is deployed to implement this node test as well as node atomization and subsequent value compar-

ison (the index key contains column data of table `doc`). At this point, the plan has evaluated the path fragment

$\odot_1::\text{closed\_auction}/\text{child}_2::\text{price}[\text{data}() > 500]$

which is still context-less. The due context is only provided by the subsequent `NLJOIN-IXSCAN` pair which verifies that the `closed_auction` elements found so far indeed are descendants of `auction.xml`’s document node. Observe that in this specific evaluation order of the location steps, the `closed_auction` nodes now assume the context node role: the plan effectively determines the `closed_auction` elements that have the document node of `auction.xml` in their ancestor axis. The reversal of axes—in this case, trading descendant for ancestor—is based on the dualities  $\text{pre} \leftrightarrow \text{pre}_o$ ,  $\text{size} \leftrightarrow \text{size}_o$  in the predicates `axis(ancestor)` and `axis(descendant)`, defined in Fig. 3. This observation applies to all other pairs of dual axes [18] (e.g., `parent/child`, `following/preceding`) and, due to the attribute encoding used in table `doc`, also to the attribute/owner relationship between element nodes and the attributes they own.

The query optimizer decides on the reordering of paths and the associated reversal of XPath axes based on its “classical” selectivity notion and the availability of eligible access paths: for a B-tree with name-prefixed keys, the RDBMS’s data distribution statistics capture tag name distribution while value-prefixed keys lead to statistics about the distribution of the (untyped) element and attribute values.

In the case of  $Q_2$ , this enabled the optimizer to decide that the access path `nkdip`, directly leading to `price` nodes (key prefix `nk`) with a typed decimal value of greater than 500 (key column `d`), is highly selective (only 9,750 of the 4.7 million nodes in the 110 MB XMark XML instance are `price` elements and only a fraction of these has a typed value in the required range).

An analogous observation about the distribution of untyped string values in the value column—the key prefix in the `vnkpv` B-tree—has led the optimizer to evaluate the general attribute value comparison

$\odot_5::\text{id}/\text{data}() = \text{doc}(\text{"auction.xml"})/\dots/\text{attribute}::\text{item}/\text{data}()$

before the “hole”  $\odot_5$  has been filled. The elements owning the `@id` attributes are resolved subsequently, effectively reversing the `attribute` axis. (This constellation repeats for the second attribute value comparison in  $Q_2$ , resumption point  $\odot_9$ .)

## 4.2 Pure SQL vs. pureXML™

With DB2 Version 9, IBM released the built-in pureXML™ XQuery processor. This opens up a chance for a particularly insightful quantitative assessment of the potential of the purely relational approach to XQuery processing discussed here: not only can a comparison with pureXML™ be performed on the same machine, but even in the context of a single query processing infrastructure (implementation of query optimizer, plan operators, and B-tree indexes).

The tree traversal of XPath location steps in pureXML™ is implemented in terms of the new XSCAN low-level plan operator. The internals of XSCAN are based on the TurboXPath algorithm [15]. This is interesting in its own right: TurboXPath supports an XPath 2.0-style dialect quite similar to Fig. 1 and, in particular, admits nested `for` loops

**Table 8: Sample query set taken from [15] (right-most column shows the query identifier used in [15]). We replaced the non-standard return-tuple ( $Q_6$ ) by an SQL/XML XMLTABLE construct.**

|       | Query   | Data  | [15] |
|-------|---|-------|------|
| $Q_3$ | /site/people/person[@id = "person0"]<br>/name/text()  | XMark | 9a   |
| $Q_4$ | //closed_auction/price/text()   | XMark | 9c   |
| $Q_5$ | /dblp/*[@key = "conf/vldb2001" and<br>editor and title]/title   | DBLP  | 8c   |
| $Q_6$ | for \$thesis in /dblp/phdthesis<br>[year < "1994" and<br>author and title]<br>return-tuple \$thesis/title,<br>\$thesis/author,<br>\$thesis/year | DBLP  | 8g   |

**Table 9: Observed result sizes and wall clock execution times (average of 10 runs).**

| Query | # nodes   | DB2 + <i>Pathfinder</i> |                       | DB2 pureXML™     |                      |
|-------|-----------|-------------------------|-----------------------|------------------|----------------------|
|       |           | stacked<br>⌚ (sec)      | join graph<br>⌚ (sec) | whole<br>⌚ (sec) | segmented<br>⌚ (sec) |
| $Q_1$ | 1,625,157 | 63.011                  | <b>11.788</b>         | 10.073           | 9.661                |
| $Q_2$ | 318       | DNF                     | <b>0.544</b>          | DNF              | DNF                  |
| $Q_3$ | 1         | 60.582                  | <b>0.017</b>          | 0.891            | 0.001                |
| $Q_4$ | 9,750     | 32.246                  | <b>0.309</b>          | 6.455            | 7.438                |
| $Q_5$ | 1         | 442.745                 | <b>0.391</b>          | 48.066           | 0.001                |
| $Q_6$ | 59        | 0.026                   | <b>0.004</b>          | 1.292            | 0.017                |

and XPath predicates, but does not implement the *full axis* feature (TurboXPath supports the vertical axes).

Aware of XSCAN’s innards, to  $Q_1$  and  $Q_2$  we added sample queries that directly stem from [15]—these queries are displayed in Table 8. Each of these queries represents a much larger query set we investigated in the course of this work—together subsuming *e.g.*, all queries of the XMark and TPox benchmark sets [17, 22]. While Queries  $Q_1$ ,  $Q_3$ ,  $Q_4$ , and  $Q_5$  are simple XPath queries, they differ in their runtime characteristics. Query  $Q_2$  is a representative for queries with value-based joins (*e.g.*, XMark Queries 8–12). DB2’s pureXML™ favors database designs that lead to comparably small XML document segments (of a few KB, say) per row. Since the tabular XML infoset encoding and XQuery processing strategy discussed here can perfectly cope with very large XML instances (beyond 100 MB), for the sake of comparison we let pureXML™ operate over both, segmented as well as monolithic XML documents.

The Queries  $Q_1$ – $Q_4$  ran against an XMark instance of 110 MB (4,690,648 nodes),  $Q_5$ ,  $Q_6$  queried an XML representation of Michael Ley’s DBLP publication database (400 MB or 31,788,688 nodes). For pureXML’s segmented document representation we cut the XMark instance into 23,000 segments of 1–6 KB and the DBLP instance into distinct publications, yielding about 1,000,000 segments of 30 nodes (ca. 800 bytes) per row. We further created an extensive XMLPATTERN index family such that at least one index was eligible to support the value references occurring in the query set (*e.g.*, for  $Q_3$  we created an index on /site/categories/category/@id).

We then translated the query set with *Pathfinder*, an

XQuery compiler that includes a faithful implementation of loop lifting and join graph isolation described in Sections 2.3 and 3. *Pathfinder* was configured to emit the SQL code derived from both, the original stacked plan and the isolated join graph. The resulting SQL queries ran against a database populated with tabular XML infoset encodings of the XMark and DBLP instances, using a B-tree index setup as described in Table 6. Both, pureXML™ and *Pathfinder* used the same DB2 UDB V9 instance hosted on a dual 3.2 GHz Intel Xeon™ computer with 8 GB of primary and SCSI-based secondary disk memory, running a Linux 2.6 kernel.

**The impact of join graph isolation.** Table 9 summarizes the average wall clock execution times we observed. Compositional compilation leads to tall stacked plans that exhibit a significant number of intermediate  $\rho$  and  $\delta$  operators. *Pathfinder* translates such plans into a SQL common table expression (WITH...) that features an equally large number of DISTINCT and RANK() OVER (ORDER BY...) clauses, leading to numerous SORT primitives in DB2 V9’s execution plans. The application of join graph isolation to such plans can have drastic effects: for Query  $Q_1$ , for example, the join graph (Fig. 7) yields a five-fold reduction of execution time over the initial stacked plan (Fig. 4). Similarly, join graph isolation lets  $Q_2$  execute in about 1/2 second (formerly the query did not complete within 20 hours).

Table 9 further assesses how DB2 pureXML™ fares against its *Pathfinder*-driven relational self. For  $Q_1$ , the universally high execution times of about 10 seconds largely reflect the substantial effort to support serialization: the resulting node sequence contains 3,249 open\_auction elements, each being the root of a subtree containing 500 nodes on average. Query  $Q_4$  primarily relies on raw path traversal performance as no value-based index can save the query engine from visiting a significant part of the XML instance. The more than 20-fold advantage of *Pathfinder* suggests that B-tree-supported location step evaluation will remain a true challenger for the XSCAN-based implementation inside pureXML™. Queries  $Q_3$ ,  $Q_5$  (and  $Q_6$ , to some extent) yield singleton (short) node sequences and constitute the best case for the segmented pureXML™ setup: here, XMLPATTERN index lookups return a single or few RID(s), directly leading the system to small XML segment(s)—the remaining traversal effort for XSCAN then is marginal. For the whole document setup, however, an index lookup could only point to the single monolithic XML instance: XSCAN thus does all the heavy work (the wildcard \* in  $Q_5$  forces the engine to scan the entire 400 MB DBLP instance). Despite the extensive index options available to support  $Q_2$ , pureXML™ is not able to finish evaluation within 20 hours: the system appears to miss the opportunity to perform value-based selections and joins early (recall the discussion of Fig. 11) and ultimately is overwhelmed by the Cartesian product of all closed\_auction, item, and category elements. The indexes largely remain unused (the predicate price[data(.) > 500] is, in fact, evaluated second to last in the execution plan generated by pureXML™).

The sub-second execution times observed for *Pathfinder* indicate that the effort to compile into particularly simply-shaped self-join chains pays off. The DB2 V9 built-in monitor facility provides further evidence in this respect: the queries enjoy a buffer cache hit ratio of more than 90% since merely table doc and indexes fight for page slots.

## 5. MORE RELATED WORK

One key ingredient in the join graph isolation process are the rewrites that move order maintenance and duplicate elimination into tail positions. Their importance is underlined by similar optimizations proposed by related efforts [10, 20, 24]: Fernández *et al.* remove order constraints and duplicates based on the XQuery Core representation [10]—an effect achieved by Rules (5) and (14) of Fig. 5. While their rewrites suffice to remove order and duplicate constraints in XPath queries like Queries  $Q_1$ ,  $Q_3$ ,  $Q_4$ , and  $Q_5$ , the principal data structure of XQuery Core—item sequences—prohibits merging of multiple orders as in Rule (13)—necessary to optimize, *e.g.*, Query  $Q_2$ . We might, however, still benefit from the optimization in [10], as it takes XPath step knowledge into account. We currently ignore this path step information and thus may end up ordering query results on more columns than strictly necessary.

In [24], an algebra over ordered tables is the subject of order optimization. An order context framework provides *minimal ordered semantics* by removing—much like Rule (5)—superfluous *Sortby* operators. In addition, order is merged in join operators and pushed through the plan in an *Orderby Pull up* much like in Section 3. In the presence of *order-destroying* operators such as  $\delta$ , the technique of [24] however fails to propagate order information to the plan tail (cf. Rule (10)).

An extension of the tree algebra (TLC-C) in the research project Timber introduces order on a global level [20] and generates tree algebra plans. While Timber cannot handle item sequence order in general, the initial Timber-generated plans could be seen as an alternative representation of join graphs. Instead of turning the workload over to a relational database, however, Timber rewrites the plan to suit its own query engine which favors *early* duplicate elimination and sorting.

Most of the rewrites and property inference rules in the present work are an adaptation of techniques known already for more than a decade [14, 21, 23]. Representing order on a *logical* algebra level—in terms of the ranking operator  $\rho$ —is a significant deviation from previous efforts. We are not aware of further approaches that *encode order as data* and thus make order accessible to *logical* query optimization.

In the context of the MonetDB/XQuery open-source project<sup>6</sup>, isolated join graphs form the starting point for the runtime optimization of XQuery expressions [2]: sampling and “zero-investment” algorithms detect data correlation and decide for the most efficient evaluation order at runtime. This approach further improves join tree planning and overcomes selectivity misestimation issues of classical optimizers.

In Section 4.1, we have seen how a selectivity-based reordering of XPath location steps can also lead to a reversal of axes. In effect, the optimizer mimics a family of rewrites that has been developed in [18]. These rewrites were originally designed to trade reverse XPath axes for their forward duals, which can significantly enlarge the class of expressions tractable by streaming XPath evaluators. Here, instead, we have found the optimizer to exploit the duality in both directions—in fact, a *descendant* axis step has been traded for an *ancestor* step in the execution plan for  $Q_2$  (Fig. 11). The evaluation of rooted */descendant::n* steps—pervasively introduced in [18] to establish a context node set

of all elements with tag  $n$  in a document—is readily supported by the  $n$ -prefixed B-tree indexes. Since the XQuery compiler implements the *full axis* feature, it can actually realize a significant fraction of the rewrites in [18].

Although we exclusively rely on the vanilla B-tree indexes that are provided by any RDBMS kernel, cost-based join tree planning and join reordering leads to a remarkable plan versatility. In the terminology of [16], we have observed the optimizer to generate the whole variety of *Scan* (strict left-to-right location path evaluation), *Lindex* (right-to-left evaluation), and *Bindex* plans (hybrid evaluation, originating in a context node set established via tag name selection; cf. the initial `closed_auction` node test in Fig. 11).

The path branching and stitching capability (Section 4.1) makes the present XQuery compilation technique a distant relative of the larger family of *holistic twig join* algorithms [6, 7, 8]. We share the language dialect of Fig. 1—coined *generalized tree pattern* queries in [6, 8]—but add to this the *full axis* feature. Quite differently, though, we (1) let the RDBMS shoulder 100% of the evaluation-time and parts of the compile-time effort invested by these algorithms (*e.g.*, the join tree planner implements the *findOrder*( $\cdot$ ) procedure of [8] for free), and (2) use built-in B-tree indexes over table-shaped data where *TwigStack* [6] and *Twig<sup>2</sup>Stack* [7] rely on special-purpose runtime data structures, *e.g.*, chains or hierarchies of linked stacks and modified B-trees, which call for significant invasive extensions to off-the-shelf database kernels.

## 6. WORK IN FLUX

This work rests on the maturity and versatility of database technology for strictly table-shaped data, resulting from 30+ years of experience. We (1) discussed relational encodings of the true XQuery semantics that are accessible for today’s SQL query optimizers, but (2) also saw that some care is needed to unlock the potential of a set-oriented query processor.

The scope of the present work reaches beyond XQuery. Tall stacked plan shapes with scattered distributions of  $\rho$  operators (Fig. 4) also are an artifact of the compilation of complex SQL/OLAP queries (in which functions of the `RANK()` family are pervasive). The observations of Section 4 suggest that the rewriting procedure of Fig. 5 can benefit commercial query optimizers also in this domain.

**Acknowledgments.** This research is supported by the German Research Council (DFG) under grant GR 2036/2-2.

## 7. REFERENCES

- [1] DB29 for Linux, UNIX and Windows Manuals, 2007. <http://www.ibm.com/software/data/db2/udb/>.
- [2] R. Abdel Kader, P. Boncz, S. Manegold, and M. van Keulen. ROX: run-time optimization of XQueries. In *Proc. SIGMOD*, 2009.
- [3] A. Arion, V. Benzaken, I. Manolescu, and A. Pugliese. Structured Materialized Views for XML Queries. In *Proc. VLDB*, 2007.
- [4] S. Boag, D. Chamberlin, and M. Fernández. XQuery 1.0: An XML Query Language. W3 Consortium, 2007. <http://www.w3.org/TR/xquery/>.
- [5] P. A. Boncz, T. Grust, M. van Keulen, S. Manegold, J. Rittinger, and J. Teubner. MonetDB/XQuery: A Fast XQuery Processor Powered by a Relational Engine. In *Proc. SIGMOD*, 2006.

<sup>6</sup><http://www.monetdb-xquery.org/>

$$\begin{array}{c}
\frac{}{\Gamma; \text{loop} \vdash \text{doc}(uri) \Rightarrow} \text{(Doc)} \quad \frac{\Gamma; \text{loop} \vdash e \Rightarrow q}{\Gamma; \text{loop} \vdash \text{fs:ddo}(e) \Rightarrow \varrho_{\text{pos:}\langle \text{item} \rangle}(\delta(\pi_{\text{iter}, \text{item}}(q)))} \text{(DDO)} \\
\frac{\{\dots, \$v_i \mapsto q_{v_i}, \dots\}; \text{loop} \vdash e_{if} \Rightarrow q_{if} \quad \text{loop}_{if} \equiv \delta(\pi_{\text{iter}_1: \text{iter}}(q_{if}))}{\{\dots, \$v_i \mapsto \pi_{\text{iter}, \text{pos}, \text{item}}(\text{loop}_{if} \bowtie_{\text{iter}_1 = \text{iter}} q_{v_i}), \dots\}; \text{loop}_{if} \vdash e_{then} \Rightarrow q} \text{(IF)} \quad \frac{\otimes \in \{=, !=, <, <=, >, >=\}}{\Gamma; \text{loop} \vdash e \otimes val \Rightarrow} \text{(VALCOMP)} \\
\frac{}{\{\dots, \$v_i \mapsto q_{v_i}, \dots\}; \text{loop} \vdash \text{if}(\text{fn:boolean}(e_{if})) \text{ then } e_{then} \text{ else } () \Rightarrow q} \\
\frac{\otimes \in \{=, !=, <, <=, >, >=\} \quad \Gamma; \text{loop} \vdash e_1 \Rightarrow q_1 \quad \Gamma; \text{loop} \vdash e_2 \Rightarrow q_2}{q \equiv (\text{doc} \bowtie_{\text{pre}=\text{item}} q_1) \bowtie_{\text{iter}=\text{iter}_1} (\pi_{\text{iter}_1: \text{iter}, \text{value}_1: \text{value}}(\text{doc} \bowtie_{\text{pre}=\text{item}} q_2))} \text{(COMP)} \quad \frac{\Gamma; \text{loop} \vdash e_{bind} \Rightarrow q_{bind}}{\Gamma + \{\$x \mapsto q_{bind}\}; \text{loop} \vdash e_{ret} \Rightarrow q} \text{(LET)} \\
\frac{}{\Gamma; \text{loop} \vdash e_1 \otimes e_2 \Rightarrow @_{\text{item}:1} (@_{\text{pos}:1}(\delta(\pi_{\text{iter}}(\sigma_{\text{value}=\text{value}_1}(q)))))} \\
\frac{\{\dots, \$v_i \mapsto q_{v_i}, \dots\}; \text{loop} \vdash e_{in} \Rightarrow q_{in} \quad q_{\$x} \equiv \#_{\text{inner}}(q_{in}) \quad \text{map} \equiv \pi_{\text{outer:iter, inner, sort:pos}}(q_{\$x})}{\{\dots, \$v_i \mapsto \pi_{\text{iter:inner, pos, item}}(\text{map} \bowtie_{\text{outer}=\text{iter}} q_{v_i}), \dots\} + \{\$x \mapsto @_{\text{pos}:1}(\pi_{\text{iter:inner, item}}(q_{\$x}))\}; \pi_{\text{iter:inner}}(\text{map}) \vdash e_{ret} \Rightarrow q} \text{(FOR)} \quad \frac{}{\{\dots, \$x \mapsto q, \dots\}; \text{loop} \vdash \$x \Rightarrow q} \text{(VAR)} \\
\frac{}{\{\dots, \$v_i \mapsto q_{v_i}, \dots\}; \text{loop} \vdash \text{for } \$x \text{ in } e_{in} \text{ return } e_{ret} \Rightarrow} \\
\frac{}{\pi_{\text{iter:outer, pos:pos}_1, \text{item}}(\varrho_{\text{pos}_1: \langle \text{sort, pos} \rangle}(q \bowtie_{\text{iter}=\text{inner}} \text{map}))} \\
\frac{}{\Gamma; \text{loop} \vdash e \Rightarrow q} \text{(STEP)} \\
\frac{}{\Gamma; \text{loop} \vdash e/\alpha::n \Rightarrow \varrho_{\text{pos:}\langle \text{item} \rangle}(\pi_{\text{iter}, \text{item}: \text{pre}}(\sigma_{\text{kindt}(n) \wedge \text{namet}(n)}(\text{doc}) \bowtie_{\alpha}(\alpha) (\pi_{\text{iter}, \text{pre}_0: \text{pre}, \text{size}_0: \text{size}, \text{level}_0: \text{level}}(\text{doc} \bowtie_{\text{pre}=\text{item}} q))))}
\end{array}$$

**Figure 13: Rules defining the compilation scheme  $\Gamma; \text{loop} \vdash e \Rightarrow q$  from XQuery expression  $e$  to algebraic plan  $q$ .**

- [6] N. Bruno, N. Koudas, and D. Srivastava. Holistic Twig Joins: Optimal XML Pattern Matching. In *Proc. SIGMOD*, 2002.
- [7] S. Chen, H. Li, J. Tatemura, W. Hsiung, D. Agrawal, and K. Selçuk Candan. Twig<sup>2</sup>Stack: Bottom-Up Processing of Generalized-Tree-Pattern Queries over XML Documents. In *Proc. VLDB*, 2006.
- [8] Z. Chen, H. Jagadish, L. Lakshmanan, and S. Pappas. From Tree Patterns to Generalized Tree Patterns: On Efficient Evaluation of XQuery. In *Proc. VLDB*, 2003.
- [9] D. Draper, P. Fankhauser, M. Fernández, A. Malhotra, K. Rose, M. Rys, J. Siméon, and P. Wadler. XQuery 1.0 and XPath 2.0 Formal Semantics. W3 Consortium, 2007. <http://www.w3.org/TR/xquery-semantics/>.
- [10] M. Fernández, J. Hidders, P. Michiels, J. Siméon, and R. Vercaemmen. Optimizing Sorting and Duplicate Elimination in XQuery Path Expressions. In *Proc. DEXA*, 2005.
- [11] G. Graefe. Sorting and Indexing with Partitioned B-Trees. In *Proc. CIDR*, 2003.
- [12] T. Grust, S. Sakr, and J. Teubner. XQuery on SQL Hosts. In *Proc. VLDB*, 2004.
- [13] T. Grust, J. Teubner, and M. van Keulen. Accelerating XPath Evaluation in Any RDBMS. *ACM TODS*, 29(1), 2004.
- [14] M. Jarke and J. Koch. Query Optimization in Database Systems. *ACM Computing Surveys*, 1984.
- [15] V. Josifovski, M. Fontoura, and A. Barta. Querying XML Streams. *VLDB Journal*, 14(2), 2004.
- [16] J. McHugh and J. Widom. Query Optimization for XML. *VLDB Journal*, 1999.
- [17] M. Nicola, I. Kogan, and B. Schiefer. An XML Transaction Processing Benchmark. In *Proc. SIGMOD*, 2007.
- [18] D. Olteanu, H. Meuss, T. Furche, and F. Bry. XPath: Looking Forward. In *Proc. XMLDM (EDBT Workshop)*, 2002.
- [19] P. E. O’Neil, E. J. O’Neil, S. Pal, I. Cseri, G. Schaller, and N. Westbury. ORDPATHS: Insert-Friendly XML Node Labels. In *Proc. SIGMOD*, 2004.
- [20] S. Pappas and H. V. Jagadish. Pattern tree algebras: sets or sequences? In *Proc. VLDB*, 2005.
- [21] H. Pirahesh, J. M. Hellerstein, and W. Hasan. Extensible/Rule Based Query Rewrite Optimization in Starburst. In *Proc. SIGMOD*, 1998.
- [22] A. Schmidt, F. Waas, M. Kersten, M. Carey, I. Manolescu, and R. Busse. XMark: A Benchmark for XML Data Management. In *Proc. VLDB*, 2002.
- [23] D. E. Simmen, E. J. Shekita, and T. Malkemus. Fundamental Techniques for Order Optimization. In *Proc. SIGMOD*, 1996.
- [24] S. Wang, E. A. Rundensteiner, and M. Mani. Optimization of Nested XQuery Expressions with Orderby Clauses. *DKE Journal*, 2006.

## APPENDIX

### A. INFERENCE RULES

The inference rule set of Fig. 13 (adopted from [12]) implements a loop-lifting XQuery compiler for the XQuery subset in Fig. 1 taking into account the XML encoding sketched in Section 2. The rule set defines a judgment

$$\Gamma; \text{loop} \vdash e \Rightarrow q,$$

indicating that the XQuery expression  $e$  compiles into the algebraic plan  $q$ , given

- (1)  $\Gamma$ , an environment that maps XQuery variables to their algebraic plan equivalent, and
- (2)  $\text{loop}$ , a table with a single column  $\text{iter}$  that invariantly contains  $n$  arbitrary but distinct values if  $e$  is evaluated in  $n$  loop iterations.

An evaluation of the judgment  $\varnothing; \boxed{\text{iter}} \vdash e_0 \Rightarrow q_0$  invokes the compiler for the top-level expression  $e_0$  (the singleton  $\text{loop}$  relation represents the single iteration of a pseudo loop wrapped around  $e_0$ ). The inference rules pass  $\Gamma$  and  $\text{loop}$  top-down and synthesize the plan  $q_0$  in a bottom-up fashion. A serialization operator at the plan root completes the plan to read  $\varphi_{\text{item}, \text{pos}}(q_0)$ .